

The QCD Critical End Point Under Strong Magnetic Fields

Sidney S. Avancini,¹ Débora P. Menezes,¹ Marcus B. Pinto,^{1,*} and Constança Providência²

¹*Depto de Física - CFM - Universidade Federal de Santa Catarina Florianópolis - SC - CP. 476 - CEP 88.040 - 900 - Brazil*

²*Centro de Física Computacional - Department of Physics - University of Coimbra - P-3004 - 516 - Coimbra - Portugal*

We use the three-flavor Nambu–Jona-Lasinio model, which includes strangeness and quark physical masses in the mean field approximation, to investigate the influence of strong magnetic fields on the QCD phase diagram covering the whole $T - \mu$ plane. It is found that the size of the first order transition line increases as the field strength increases so that a larger coexistence region for hadronic and quark matter should be expected for strong magnetic fields. The location of the critical end point is also affected by the presence of magnetic fields which invariably increase the temperature value at which the first order line terminates. On the other hand, the critical end point chemical potential value displays a subtle oscillation around the $B = 0$ value for magnetic fields within the $10^{17} - 10^{20}$ G range. These findings may have non trivial consequences for the physics of magnetars and heavy ion collisions.

PACS number(s): 24.10.Jv, 11.10.-z, 25.75.Nq

Magnetic catalysis is an interesting phenomenon with direct consequences on the QCD chiral symmetry breaking (CSB) mechanism. At vanishing T and μ one observes, within effective quark models, that the presence of a magnetic field (B) stabilizes the chirally asymmetric vacuum by antialigning the helicities of a quark–anti-quark pair ($\bar{q}q$) which is then bound by the strong interaction. This contrasts with the behavior of the BCS ground state of an ordinary superconductor where B favors the alignment of the spins for an electron pair opposing pair formation. As a consequence of magnetic catalysis, the quark condensate, and hence the quark effective mass, assumes higher values as B increases. Predictions based on the Nambu–Jona-Lasinio model (NJL) [1] suggest that the effective quark mass raises by approximately 30 to 40% when B increases from 10^{17} to 3×10^{19} Gauss, i.e., by about two orders of magnitude [2, 3]. It is important to stress that the effective masses at vanishing B coincide with the ones obtained for $B = 10^{17}$ G or lower. The fact that magnetic fields induce magnetic catalysis, enhancing CSB, naturally leads to the question of how these fields would influence chiral phase transitions at finite temperatures and/or chemical potentials. Of course this is more than merely an academic question since one can immediately point out at least two realistic scenarios whose physics are influenced by the behavior of strongly interacting matter under intense magnetic fields. The first refers to the high temperature and low chemical potential regime relevant to non central heavy ion collisions where huge fields, of the order $|eB| \geq m_\pi^2 \sim 10^{18}$ G, can be created by heavy ion currents due to the spectator nucleons. The field intensity depends on the centrality and beam momentum so that $|eB| \approx 5m_\pi^2$ can be reached at RHIC while $|eB| \approx 15m_\pi^2$ can be reached at the LHC. Although time dependent and short-lived [4] these fields

may have a non negligible effect on the transition [5]. Strong magnetic fields in heavy ion collisions at beam energies ranging from 0.2 to 2 GeV/nucleon, which cover most of the accelerators in the world, were considered in [6], where the authors conclude that particles with low masses and their differential ratios (as π^-/π^+ , for example) can be used as possible probes of the density dependence of the symmetry energy, another topic of interest in the recent literature. The second scenario refers to the cold baryon-dense matter which forms compact stellar objects such as magnetars. While ordinary neutron stars bear a magnetic field of the order of $10^9 - 10^{12}$ G, magnetars, believed to be the source of intense gamma and X rays, bear fields of the order of $10^{13} - 10^{15}$ G at their surface reaching values up to 3 to 5 times of magnitude greater in their center [7]. As far as phase transitions are concerned, these two physically appealing situations are located at the high- T –low- μ (relativistic heavy ion collisions) and low- T –high- μ (neutron stars) extremes of the QCD phase diagram while the intermediate region lies within the capabilities of experiments such as the low energy scan in HIC at RHIC, FAIR at GSI, NICA at JINR, and J-PARC at JAERI where, eventually, high magnetic fields will also be reached.

The determination of the QCD phase diagram, even at vanishing B , is still a matter of great theoretical and experimental activities. In this case, powerful lattice simulations have established that at vanishing baryon densities there is no true phase transition from hadronic matter to a quark gluon-plasma but rather a very rapid raise in the energy density signaling a crossover characterized by a pseudocritical temperature, T_{pc} , which is expected to be within the 150–200 MeV range, with systematic errors [5]. The situation is less clear for the finite chemical potential region since, so far, there is no reliable information available from lattice QCD evaluations. Nevertheless, most finite μ lattice extrapolations for the $\mu = 0$ Columbia plot indicate that the critical first order surface (on the $m_{u,d} - m_s - \mu$ plane) will hit the physical current mass values at some finite μ thereby characterizing a critical end point (CEP) [8].

Therefore, the use of effective models for QCD consti-

*Electronic address: marcus@fsc.ufsc.br

tutes the pragmatic approach to treat the finite chemical potential region, especially at very low temperatures. Within this spirit, the three-flavor version of the NJL has been widely used in investigations which aim to analyze the phase structure of chiral transitions. Using a standard parametrization, at $B = 0$, this model predicts a phase diagram [9] which is in accordance with what is the most general current belief. Namely, the model predicts that at vanishing chemical potential a crossover takes place with a T_{pc} which is in good agreement with the lattice results. At zero temperature, a first order transition occurs for $\mu \sim M_B/3$, where M_B is the baryon mass, so that a first order transition line emerges at smaller μ as T departs from zero. Since at $\mu \cong 0$ a crossover is predicted, this line cannot cover the whole $T - \mu$ plane and will terminate at a CEP located at intermediate values of T and μ . Considering this picture as the $B = 0$ benchmark one can further analyze how a magnetic field will influence the expected QCD chiral transition. So far, most model applications carried out with this aim were performed at $\mu = 0$ with the two-flavor linear σ model (LSM) [10] as well as with the two-flavor NJL model [11] predicting that the crossover takes place at higher T_{pc} when $B \neq 0$. Another interesting outcome from these investigations shows that the chiral and deconfining lines can split at finite B when the models also include the Polyakov loop. On the lattice side, a two flavor simulation, which used quark current masses corresponding to pion masses on the range 200-400 MeV has shown that the deconfinement and chiral symmetry raise by just a few percent even for very high fields and have not observed any splitting [12]. However, very recently another lattice simulation has considered 2+1 flavors and physical values for the quark current masses predicting that the pseudo critical temperature should decrease with increasing B [5]. This also constitutes an interesting result if one recalls that the running of the strong coupling in the presence of B may turn the magnetic catalysis effect around, as suggested in Ref. [13].

Despite the progress made at vanishing baryon density very little has been done to determine the influence of magnetic fields on the whole $T - \mu$ plane. One such investigation was carried out in Ref. [14] using the standard two flavor LSM but when the vacuum is included, as it should be [10], the whole $T - \mu$ plane is dominated by the crossover just as it happens at $B = 0$. On the contrary, as shown in [15], the standard two flavor version of the NJL model in the chiral limit does not share this property allowing for the observation of how a magnetic field influences the location of the tricritical point. In Ref. [15] a Fock-Schwinger proper time method was used in the chiral limit. The authors have observed a curious pattern between magnetic catalysis and the Haas-van Alphen effect, which leads to oscillations in the first order transition line. The complexity of the phase diagram obtained with several tricritical points is probably due to the zero mass quark limit and further investigation with realistic current quark masses is needed. As

emphasized in [16], strange quarks play a crucial role in shaping the phase diagram of QCD since their mass, m_s , controls the nature of the chiral and deconfinement transition. At the same time, this mass has also an important effect on the stability limit of neutron stars and on the possible existence of a quark core in collapsed stars. For these objects, the establishment of the critical first order line is of utmost importance once the possibility for hybrid and quark star formation depends on the quark matter nucleation process. The determination of the first order line, at $B \neq 0$, may also be relevant in the framework of studies related to thermal nucleation of quark droplets in hadronic matter found in protoneutron stars whose temperatures are of the order 10–20 MeV.

In this Letter we report on the main results obtained by scanning the whole $T - \mu$ plane paying special attention to the CEP and to the first order coexistence region. We do not consider the Polyakov loop since its effects are more pronounced at the high temperature and low chemical potential region [10, 11]. In [17] it was shown that, although it changes considerably the values of the temperature and chemical potential related to the CEP, the qualitative behavior of the phase transition was not modified.

By mapping the first order line on the $T - \mu$ plane we can automatically predict the location of the CEP for different values of B . At vanishing μ we reproduce the results known from the other model applications (like those in Refs. [10, 11]) predicting that the $B = 0$ crossover will take place at a higher T_{pc} for $B \neq 0$. The new results reported here emerge at the finite baryonic density domain where we observe that the presence of a magnetic field favors the presence of latent heat at higher temperatures, invariably increasing the size of the first order transition region so that the CEP temperature, $T_{CEP}(B)$, increases with B . We also show that the critical chemical potential, $\mu_{crit}(B)$, which determines the low temperature first order transition displays a non trivial behavior moving around the $B = 0$ value for magnetic fields in the range $10^{17} - 10^{20}$ G. To the best of our knowledge this is the first time such predictions are made within a more realistic approach, which takes strangeness and physical masses into account.

In order to consider (three flavor) quark matter subject to strong magnetic fields we introduce the following Lagrangian density

$$\mathcal{L} = \mathcal{L}_f - \frac{1}{4}F_{\mu\nu}F^{\mu\nu}, \quad (1)$$

where the quark sector is described by the su(3) version of the Nambu–Jona-Lasinio model which includes scalar-pseudoscalar and the t’Hooft six fermion interaction that models the axial $U(1)_A$ symmetry breaking [18]:

$$\mathcal{L}_f = \bar{\psi}_f [\gamma_\mu (i\partial^\mu - q_f A^\mu) - \hat{m}_c] \psi_f + \mathcal{L}_{sym} + \mathcal{L}_{det}, \quad (2)$$

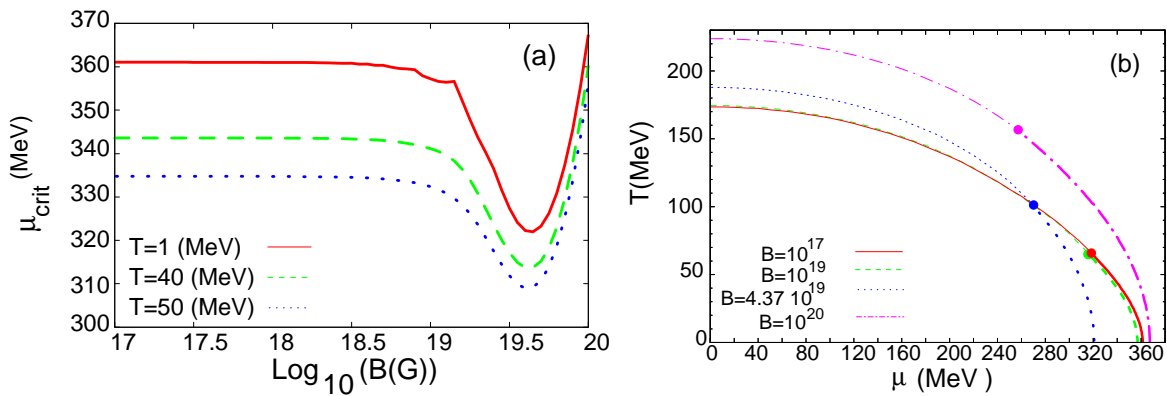


FIG. 1: a) Critical chemical potential in terms of the magnetic field for different values of the temperature; b) Phase diagram on the $T - \mu$ plane. The thick curves represent first order transition lines which terminate at a critical end point identified with a full dot and the thin lines represent a crossover.

with \mathcal{L}_{sym} and \mathcal{L}_{det} given by [19]:

$$\mathcal{L}_{\text{sym}} = G \sum_{a=0}^8 [(\bar{\psi}_f \lambda_a \psi_f)^2 + (\bar{\psi}_f i \gamma_5 \lambda_a \psi_f)^2], \quad (3)$$

$$\mathcal{L}_{\text{det}} = -K \left\{ \det_f [\bar{\psi}_f (1 + \gamma_5) \psi_f] + \det_f [\bar{\psi}_f (1 - \gamma_5) \psi_f] \right\}, \quad (4)$$

where $\psi_f = (u, d, s)^T$ represents a quark field with three flavors, $\hat{m}_c = \text{diag}_f(m_u, m_d, m_s)$ is the corresponding (current) mass matrix while q_f represents the quark electric charge, $\lambda_0 = \sqrt{2/3}I$ where I is the unit matrix in the three flavor space, and $0 < \lambda_a \leq 8$ denote the Gell-Mann matrices. The model is not renormalizable, and as a regularization scheme for the divergent ultraviolet integrals we use a sharp cut-off, Λ , in 3-momentum space. The parameters of the model, Λ , the coupling constants G and K and the current quark masses m_u^0 and m_s^0 are determined by fitting f_π , m_π , m_K and $m_{\eta'}$ to their empirical values. Throughout this paper we consider $\Lambda = 631.4 \text{ MeV}$, $m_u = m_d = 5.5 \text{ MeV}$, $m_s = 135.7 \text{ MeV}$, $G\Lambda^2 = 1.835$ and $K\Lambda^5 = 9.29$ as in [20].

As usual, A_μ and $F_{\mu\nu} = \partial_\mu A_\nu - \partial_\nu A_\mu$ are used to account for the external magnetic field. We consider a static and constant magnetic field in the z direction, $A_\mu = \delta_{\mu 2} x_1 B$.

The thermodynamical potential for the three flavor quark sector, Ω_f is written as

$$\Omega_f(T, \mu, B) = 2G \sum_{i=u, d, s} \phi_i^2 - 4K \phi_i \phi_j \phi_k + \left(\Omega_f^{\text{vac}} + \Omega_f^{\text{mag}} + \Omega_f^{\text{med}} \right), \quad (5)$$

where the vacuum (Ω_f^{vac}), the magnetic (Ω_f^{mag}), the medium contributions (Ω_f^{med}) and the condensates ϕ_i have been evaluated with great detail in Ref. [2, 3]. The effective quark masses are solutions of the gap equations

obtained from the minimization of the thermodynamic potential with respect to the effective masses,

$$M_i = m_i - 4G\phi_i + 2K\phi_j\phi_k, \quad (6)$$

with (i, j, k) being any permutation of (u, d, s) . In this work we consider $\mu = \mu_u = \mu_d = \mu_s$.

The first order phase transition line is obtained by enforcing the Gibbs conditions while the cross over region is determined by the maximum of $-\phi_m/dT$ ($m = u, d$).

In Fig. 1a we plot the critical chemical potential as a function of the magnetic field for different low temperature values where the first order transitions take place. For a fixed magnetic field, the critical chemical potential (μ_{crit}) is approximately constant up to magnetic fields of the order of 10^{19} G, where it reduces drastically reaching a minimum value around 3×10^{19} G and then it increases again. This occurs precisely when just one Landau level is filled. One can clearly see the effects of the filling of the Landau levels at low temperatures, where the van Alphen oscillations are seen.

The effects of the behavior observed in Fig. 1a are reflected in the curves shown in Fig. 1b, where a $T - \mu$ phase diagram is shown for different values of B . As the magnetic field increases, the line of the first order phase transition also increases. The line moves towards a lower chemical potential and then back to higher chemical potentials for increasing values of B . The highest point in each first order transition curve is the CEP, indicated with a full dot. The curve obtained for $B = 10^{17}$ G coincides exactly with the results presented in [9] for a zero magnetic field. The pattern observed in Fig. 1b can be seen with more detail in Fig. 2 where the dependence of μ_{CEP} and T_{CEP} , which characterize the CEP, are shown as a function of the magnetic field B . Fig. 2a shows that μ_{CEP} essentially decreases with B , with a lower decrease for fields stronger than 10^{19} G. Just below 10^{20} G, μ_{CEP} starts to increase. Fig. 2b represents μ_{CEP} versus T_{CEP} , each point corresponding to a different value of the magnetic field: the smallest value of the

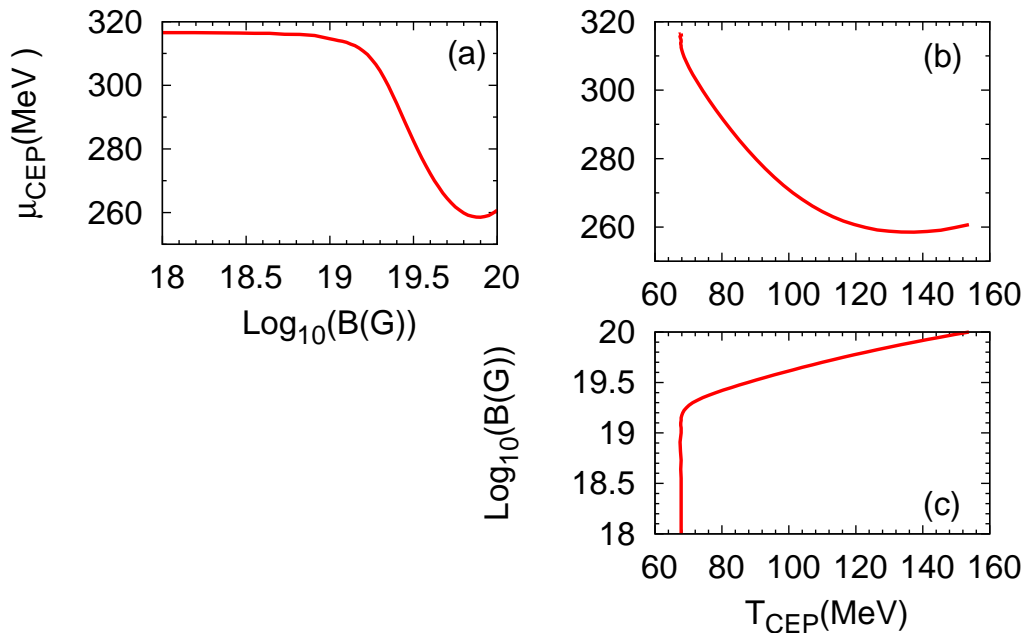


FIG. 2: Critical end point chemical potential μ_{CEP} in terms of a) the magnetic field, and b) the critical end point temperature T_{CEP} ; c) T_{CEP} as a function of B .

critical chemical potential, 258.5 MeV, corresponding to a $T_{CEP} \simeq 137$ MeV occurs for $B = 8 \times 10^{19}$. On the other hand, T_{CEP} always increases with the increase of B , mainly above 10^{19} G.

In summary, our results show that, at $\mu = 0$, T_{pc} increases with B in agreement with most model calculations [10, 11] and an early lattice simulation [12] which is not surprising since we are dealing with the NJL within the MFA. On the other hand, the main contribution of our work concerns the critical end point and the first order coexistence region for which magnetic effects become noticeable for fields greater than 10^{17} G. In this case, one observes an increase on the size of the first order transition line with T_{CEP} moving to higher values as B increases. This result can be of interest for the physics of heavy ion collisions at intermediate energies. We have also observed that, due to the van Alphen effect, the first order transition lines display a non trivial behavior oscillating around the $B = 0$ line. This implies that, as

B increases, criticality will be achieved at chemical potential values which can be greater or smaller than the $B = 0$ value, $\mu_{crit} \simeq 360$ MeV. These findings may have direct consequences regarding the dynamics of the first order phase transition which influences the quark matter nucleation process. Although we have attempted to perform a realistic application, by considering three quark flavor and physical mass values, it is important to recall that at temperatures higher than 100 MeV the effects of the Polyakov loop may be important [21]. The Polyakov loop field is going to be more carefully considered in a forthcoming paper but we believe that these seminal qualitative results are not going to be altered.

Acknowledgements: This work was partially supported by the Capes/FCT n. 232/09 bilateral collaboration, by CNPq and FAPESC (Brazil), by FCT and FEDER (Portugal) under the project PTDC/FIS/113292/2009 and by Compstar, an ESF Research Networking Programme.

[1] Y. Nambu and G. Jona-Lasinio, Phys. Rev. **122**, 345 (1961); **124**, 246 (1961).
[2] D.P. Menezes, M.B. Pinto, S.S. Avancini, A. Pérez Martínez and C. Providência, Phys. Rev. **C 79**, 035807 (2009); D.P. Menezes, M.B. Pinto, S.S. Avancini and C. Providência, Phys. Rev. **C 80**, 065805 (2009).
[3] S.S. Avancini, D.P. Menezes and C. Providência, Phys. Rev. **C 83**, 065805 (2011).

[4] K. Fukushima, D. E. Kharzeev and H. J. Warringa, Phys. Rev. **D 78**, 074033 (2008); D. E. Kharzeev and H. J. Warringa, Phys. Rev. **D 80**, 0304028 (2009); D. E. Kharzeev, Nucl. Phys. **A 830**, 543c (2009).
[5] G.S. Bali, F. Bruckmann, G. Endrödi, Z. Fodor, S.D. Katz, S. Krieg, A. Schäfer and K.K. Szabó, arXiv: 1111.4956 [hep-lat].
[6] Li Ou and Bao-An Li, arXiv:1107.3192v1[nucl-th].

- [7] R. Duncan and C. Thompson, *Astron. J.*, **32**, L9 (1992); astro-ph/0002442; C. Kouveliotou et al, *Nature* **393**, 235 (1998).
- [8] K. Fukushima and T. Hatsuda, arXiv: hep-ph/1005.4814.
- [9] P. Costa, M.C. Ruivo and C.A. de Sousa, *Phys. Rev. D* **77**, 096001 (2008).
- [10] A.J. Mizher, M.N.Chernoub and E.S. Fraga, *Phys. Rev. D* **82** 105016 (2010); V. Skokov, arxiv: hep-ph/1112.5137.
- [11] R. Gatto and M. Ruggieri, *Phys. Rev. D* **83**, 034016, K. Fukushima, M. Ruggieri and R. Gatto, *ibid.* **81** 114031 (2010); R. Gatto and M. Ruggieri, *ibid* **82**, 054027 (2010).
- [12] M. D'Elia, S. Mukherjee and F. Sanfilippo, *Phys. Rev. D* **82**, 051501 (2010).
- [13] V.A. Miransky and I.A. Shokov, *Phys. Rev. D* **66**, 045006 (2002).
- [14] J.O. Andersen and R. Khan, arXiv: hep-ph/1105.1290v3.
- [15] T. Inagaki, D. Kimura and T. Murata, *Prog. of Theo. Phys.* **111**, 371 (2004).
- [16] B. Müller, nucl-th/1112.5382
- [17] P. Costa, C.A. de Souza, M.C. Ruivo and H. Hansen, *Europhys. Lett.* **86**, 31001 (2009).
- [18] T. Hatsuda, T. Kunihiro, *Phys. Lett. B* **198**, 126 (1987); S.P. Klevansky, *Rev. Mod. Phys.* **64**, 649 (1992). 649.
- [19] M. Buballa, *Phys. Rep.* **407**, 205 (2005).
- [20] T. Hatsuda and T. Kunihiro, *Phys. Rep.* **247**, 221 (1994).
- [21] P. Costa, M.C. Ruivo, C.A. de Sousa and H. Hansen, *Symmetry* **2**(3), 1338 (2010); arXiv:1007.1380 [hep-ph].